The role of individual chains in polymer deformation*

H. H. Kausch† and C. J. G. Plummer
Department of Materials Science and Engineering, EPFL, CH-1015 Lausanne, Switzerland

The characteristic properties of molecular chains are their length, anisotropy and mobility. Although the macroscopic (mechanical) properties of polymers basically reflect these molecular characteristics, it is not always easy to identify the response of an individual molecule to stress. Much of the scientific work of Ward has been devoted to this problem and it is for this reason that some specific aspects of the stress transfer through chain molecules will be elaborated here. Thus, the representation of molecular anisotropy through aggregate models, the extreme situations of stress transfer through tie-molecules in semicrystalline fibres (shear stresses up to 3.5 GPa) and in elongational flow will be discussed. Recent results of stress transfer across interfaces in cracked homopolymers and in blends will be reviewed.

(Keywords: molecular chains; polymer deformation; stress transfer)

INTRODUCTION

It is the purpose of this paper to discuss the role of individual chains in the different phases of polymer deformation[1-5]. At small deformations one would have to analyse the elastic and anelastic response of the aggregate formed by the highly anisotropic molecules, and at very large deformations one would evidently be concerned with the conformational changes, slippage, disentanglement and scission of chains during the plastic deformation and rupture of polymers.

Real materials, especially many of the most recent developments, are highly heterogeneous. Most of their properties are determined by their collective (micro)-structure, by the nature, size and orientation of their structural units and by the quality of their interfaces. The microstructure evolves through deformation and diffusive processes. Clearly, in such materials the link between atomic structure and macroscopic properties is not direct. These principles have been recognized ever since Voigt[6] and Reuss[7] developed their respective models, which subsequently gave rise to a series of papers on the fundamentals of stress and strain distribution in heterogeneous solids[2-5,8-10] and which are still of current interest[11]. Thus the first point to be discussed is the description of heterogeneous polymer microstructure through aggregate models. Whilst this is essentially a static problem, much has been learned about the significance of the aggregating elements by the study of their orientation behaviour—and this involves molecular dynamics: orientation and relaxation are working against each other. The degree of molecular orientation achieved in uniaxial drawing of a sample depends on the time-scale of the experiment and on the intensity of the forces transmitted to a molecular segment. Thus the second subject to be discussed in this paper is that of stress transfer onto individual molecules, ranging from the extremely high shear stresses imparted onto tie-molecules in semicrystalline fibres ($\tau \sim 3.5$ GPa) to the much smaller ones in the pull-out of interdiffused chains ($\tau \sim 25$ MPa).

MOLECULAR ORIENTATION AND AGGREGATE MODELS

Polycrystalline materials are aggregates formed of small, anisotropic units, the crystallites, which generally have identical elastic properties but differ in size and orientation (*Figure 1*). The calculation of the elastic constants of such an aggregate can be approached in two ways: either by assuming homogeneous stress (the Reuss average) or uniform strain (the Voigt average). The Reuss average involves averaging the compliance constants and it is thus most appropriate to a layer-like or series arrangement of the elastic units. The Voigt average describes a parallel (columnar) arrangement of the elastic elements. These two averages provide the lower and upper bounds, respectively, for the elastic constants of a random aggregate.

While studying the optical and mechanical anisotropy of oriented crystalline polymers, Ward[1] recognized that a relation analogous to that for polycrystalline materials should exist between the elastic constants of an oriented polymer and those of its partially crystalline domains. In his classical treatment[1] he derived the elastic constants and compliances of an aggregate composed of identical anisotropic semicrystalline elements. Despite the fact that these elements are formed by crystalline and amorphous material, they are assigned the properties of one homogeneous phase, thus the representation of the body is achieved through a one-phase model. As Ward points out, the aggregate model takes no account of the way in which crystalline and amorphous material are

* Presented at 'Polymer Science and Technology—a conference to mark the 65th birthday of Professor Ian Ward FRS', 21–23 April 1993, University of Leeds, UK

† To whom correspondence should be addressed

0032-3861/94/18/3848-10

interrelated, but assumes that this relation does not change substantially as a result of stretching. Where the theory gives a reasonable fit to experimental data, it suggests strongly that orientation occurs principally through the (affine) rotation of the constitutive, semi-crystalline elements. In these calculations the interface between the elements is assigned the role of confining the orienting units and of transmitting stresses, and is assumed insensitive to the state of deformation or orientation.

The aggregate model has been discussed in detail by Ward and his collaborators in several comprehensive publications[2–5]. Here only certain key features will be cited. For example, the compliance constants S_{33} corresponding to the inverse of the axial Young's modulus of an oriented fibre or uniaxially oriented film will be given by:

$$S_{33} = I_1 s_{11} + I_2 s_{33} + I_3(2s_{13} + s_{44}) \quad (1)$$

s_{11}, s_{33}, s_{13} and s_{44} are the compliance constants of the anisotropic elastic unit, which are taken to be those of a highly oriented sample; these need not, and indeed generally will not, correspond to the theoretical values for a perfectly aligned molecular chain.

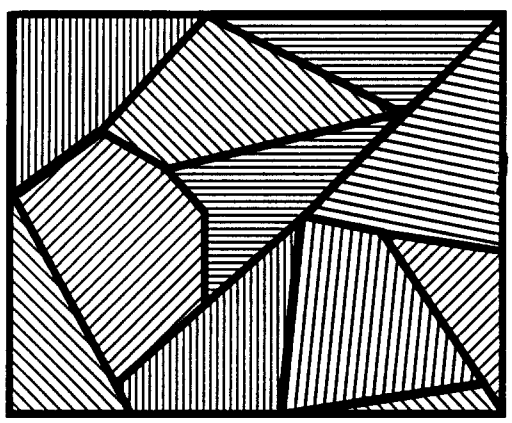

Figure 1 Two-dimensional model representation of a polycrystalline material consisting of randomly arranged 'elastic elements'. In the Voigt and Reuss approach, the shape and the size of the individual elements are without importance, only the elastic properties and the orientation distribution are taken into account

I_1, I_2 and I_3 are orientation functions, perhaps better termed orientation averages, with:

$$I_1 = \overline{\sin^4\theta} \qquad I_2 = \overline{\sin^4\theta} \qquad I_3 = \overline{\sin^2\theta\cos^2\theta} \quad (2)$$

where θ is the angle between the symmetry axis of the anisotropic elastic unit (assumed here to have fibre symmetry) and the draw direction[1–5]. Their orientation averages reflect the state of orientation.

Ward has determined the orientation functions for affine deformation at constant total volume[1] and thus the change in Young's modulus $E_{33} = 1/S_{33}$ as a function of draw ratio λ. In a later publication Kausch[8] compared E_{33} (λ) of different uniaxially oriented polymers with theoretical curves obtained from the aggregate model using the anisotropy of the elastic elements (s_{33}/s_{11}) as a parameter (*Figure 2*).

It appears from this comparison that the orienting elements in glassy amorphous polymers formed of flexible chains such as polystyrene (PS), poly(methyl methacrylate) (PMMA) and poly(vinyl chloride) (PVC), have a rather limited anisotropy (s_{33}/s_{11}) of between 0.5 and 1.0. For the semicrystalline nylon 66 with its strong hydrogen bond interactions between chains, the apparent elemental anisotropy is much larger ($s_{33}/s_{11} = 0.07$) but still below that of the molecular crystal ($s_{33}/s_{11} \sim 0.013$). However, for orienting rigid rod molecules of a thermotropic liquid crystalline polymer such as the copolymer of hydroxy benzoic acid and hydroxy naphthoic acid (HBA-HNA), the elastic anisotropy of the orienting units has been found[12–14] to be as large as 1:50 which corresponds quite well to the molecular anisotropy.

From these findings, it has been concluded that a given individual straight chain segment in a deforming matrix does not generally rotate in an affine manner. Local deformation can be non-affine, owing to segmental mobility and to the dispersed nature of the applied forces (see below). As will be discussed in the following section, chain segments are oriented efficiently only if they can be tightly gripped.

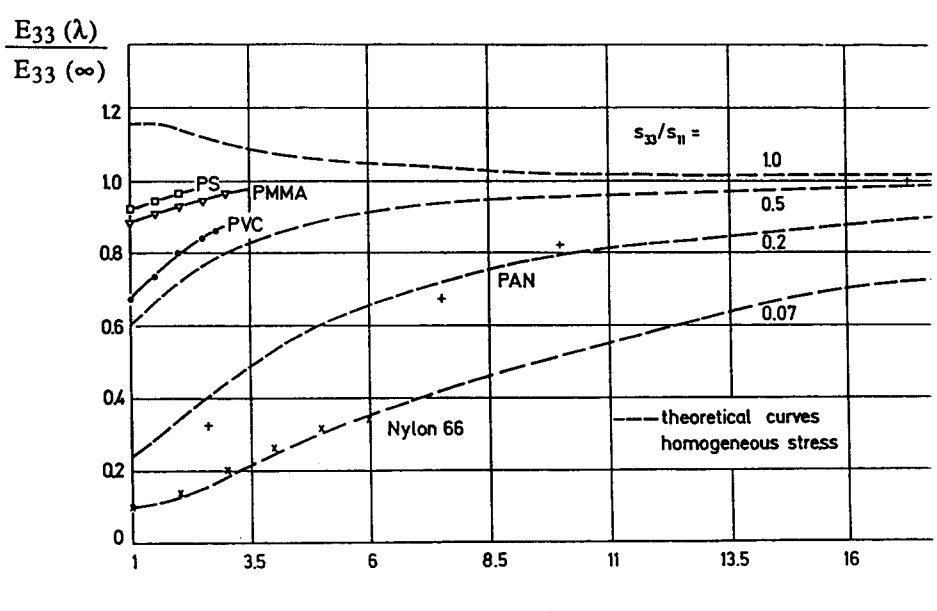

Figure 2 Comparison of experimental data for Young's modulus with theoretical curves as predicted by equation (1)

APPLICATION OF FORCES TO CHAIN MOLECULES

Mechanical forces can be applied to a given chain segment by a concentrated action on the chain ends (as in crosslinked or entangled elastomers) or by a more or less dispersed interaction between the segment and its surroundings (as in a stressed isotropic thermoplastic solid or in a flowing solution).

The intensity of stress transfer and the response of the chain segment will be substantially different in these cases. Depending on chain mobility there will be competition between chain deformation owing to external forces and chain contraction owing to entropic forces (*Figure 3*).

Forces (exclusively) transmitted through crosslinking points

The 'grip' exerted by two crosslinking points onto the interconnecting chain segment is perfect: highly localized and in no way time-dependent. The chain segment deforms as the vector between the crosslinking points, the forces encountered by the chain ends are rubber elastic, entropic at small extension ratios, energy elastic if the segment is (almost) completely extended. Chain scission occurs if the transmitted forces exceed the chain strength (~ 3 nN).

Forces transmitted onto tie-molecules through crystallites

Taut tie-molecules which are partly embedded in two different crystal lamellae of an oriented fibre will be highly stressed if the fibre is subjected to a large tensile strain. The axial fibre deformation will separate the lamellae from each other thus forcing the fully extended tie-molecules to extend even further which requires work against the lattice potential and the chain stiffness (*Figure 4*). Kausch and Langbein[15] have calculated how the (static) stresses are transferred from the (infinitely rigid) loaded crystal lamellae to an elastic tie-molecule (*Figure 5*). Gibson *et al.*[16] have further refined this model by considering the (shear) deformation of the lamella during tie pull-out.

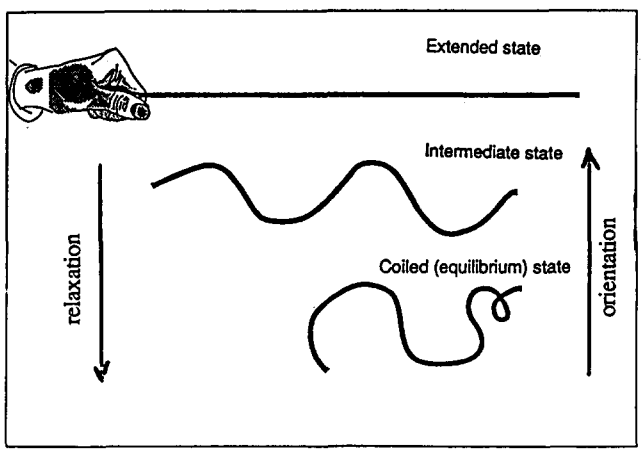

Figure 3 External forces which tend to stretch (and orient) a segment are applied through action on crosslinking or entanglement points or through shear, and relaxation occurs through disentanglement, slip, conformational changes or chain scission

Kausch and Langbein calculated the maximum tensile force (f_{max}) imposed elastically onto a polyamide 6 (PA6) tie-molecule to be 3.94 nN (which corresponds to a tensile stress of 22.4 GN m^{-2}). The 'grip' is exerted by the periodic variations of the lattice potential which is strongest at the sites of the hydrogen bonds (CO–NH groups). This is a rather important point which justifies some deliberation. The axial displacement of a segment within a homogeneous attractive potential would require no force at all. If the segment, say a CH_2 group of length Δl, were to be pulled from a homogeneous A-phase into a homogeneous B-phase of smaller cohesive energy (E_{coh}), however, then a force of $f = \Delta E_{coh}/\Delta l$, would be necessary to achieve the displacement across the phase boundary. Using a ΔE_{coh} value of 2.77 kJ (mol CH_2)$^{-1}$ for the difference between crystalline and amorphous polyethylene (PE), a force of only 0.037 nN would be necessary for the pull-out of a CH_2 group from an assumed homogeneous lattice potential as opposed to 0.087 nN for the pull-out of a CH_2 group from a crystal with a periodic lattice potential[9].

The efficiency of stress-transfer through elastic displacement of a segment with respect to its surroundings mainly depends, therefore, on the existence of spatial potential variations and on their correlation with respect to the pulled chain. In fact the stress decay observed in PA6 (*Figure 5*) between -0.630 nm and 0.868 nm (location of the first CO-NH group from the crystal boundary) is equivalent to the action of a shear stress of 3.4 GN m^{-2} on a cylinder with a diameter of 0.48 nm which has the same cross-section as a PA molecule. Even the average shear stress taken over the total molecular stress decay length of 2.5 nm amounts to ~ 1.0 GN m^{-2} which is 20 to 50 times the shear stress transmitted in shear from a PA6 matrix to a glass fibre.

Forces transmitted between amorphous segments

As already discussed in the previous section, the lack of spatial correlation in an amorphous phase greatly reduces the fluctuations of the attractive potential to

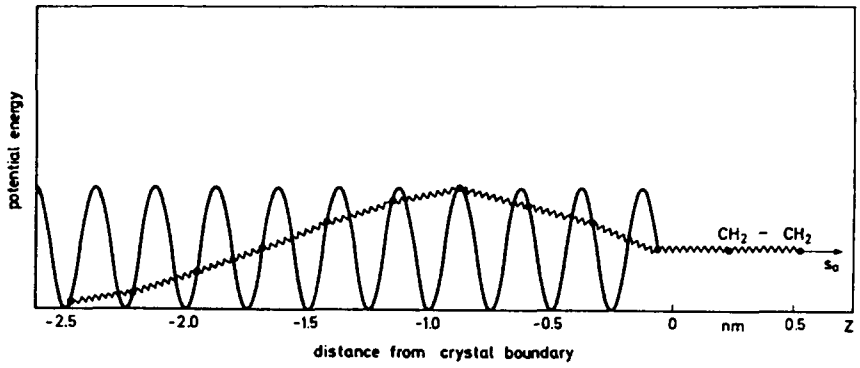

Figure 4 Schematic representation of the pull-out of a PE tie-molecule from a crystallite

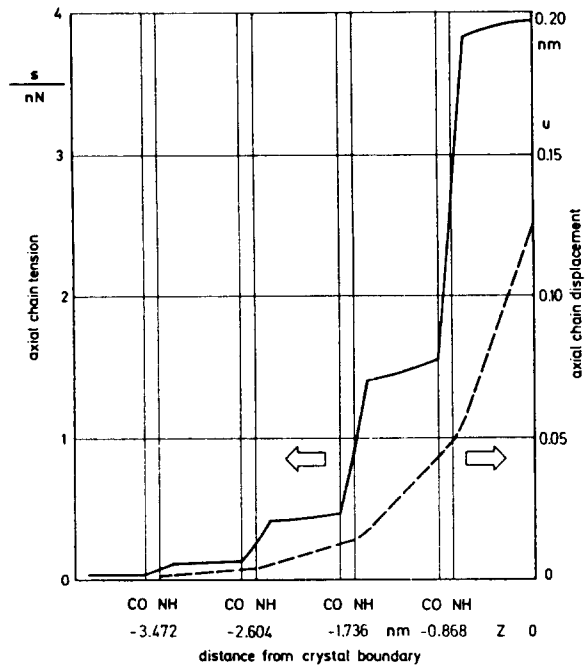

Figure 5 Axial tension and displacement of a stressed tie-molecule in a PA6 crystal

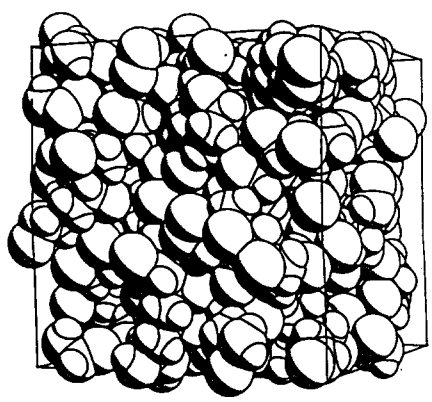

Figure 6 Energy minimized structure of an amorphous polymer [poly(vinyl chloride)] inside a periodic box (degree of polymerization = 200). (Courtesy of Professor U. W. Suter, ETH-Zürich)

which a given segment is exposed. In addition, the molecules have a random conformation which means that the fully extended straight *trans* sections are rather short; kinked (*tgt*), bent or even folded conformations dominate (*Figure 6*). In such a situation, stress accumulation at a given segment can easily be avoided by lateral displacement, bond rotation (*g-t* transformation) and bending of the segment. Others[17-19] have studied this process in detail using computer simulation techniques. In a first step they randomly packed chains into a 'cell' of given volume constantly minimizing the total potential energy of the system. A typical amorphous structure thus obtained is shown in *Figure 6*. In a second reiterative process they deformed this structure and again established the configuration of minimum energy. In doing this they noted three remarkable facts, the first being that the initial von Mises shear resistance of a system with fixed boundaries is not zero, but finite, at 50 MPa. This is not an artefact, but a manifestation of the finiteness of the system; for a system of this small size subjected to periodic boundary conditions the average value of the initial disorder related to local atomic stresses does not vanish. Mott *et al.*[18] have termed this an atomic level 'stress noise'. As the system size is increased or as an ensemble average is obtained of a larger number of systems the level of the atomic stress noise decreases predictably with the square root of the number of elements in the ensemble, or the size of the system.

The second observation concerns the initial soft reversible anelastic behaviour of the system with a slope considerably less than the elastic loading line shown in *Figure 7* as the dashed reference line. The first displacement steps were easily accommodated by the amorphous structure by slight positional changes not involving any plastic deformation, or indeed any conformational changes or segmental slip. Only after the internal elastic stresses had substantially accumulated locally (for a small volume element, to a point far beyond the yield stress) plastic events took place, accompanied by sudden drops in stress (marked a and b in *Figure 7*). However, a plastic event was never limited to one well confined site such as a

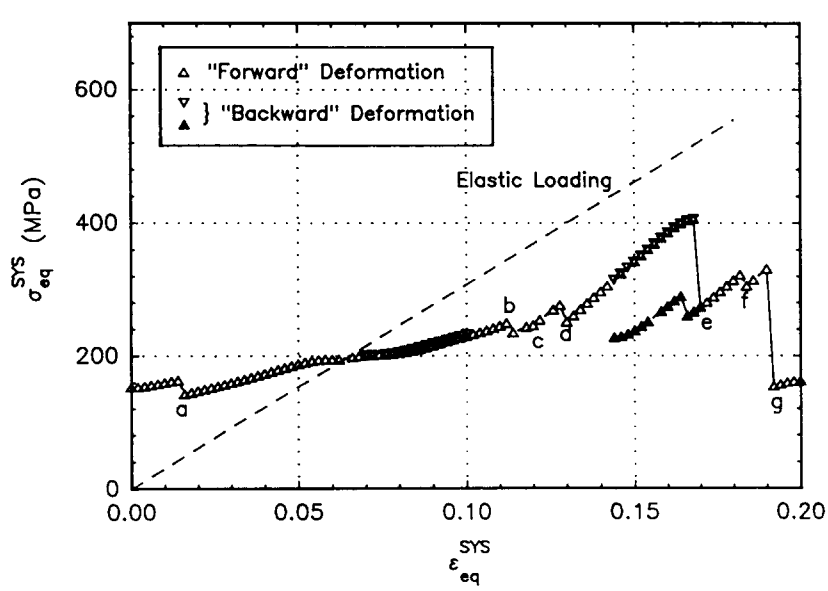

Figure 7 System stress–strain behaviour for a single representative structure. The structure was deformed in axial extension. The 'elastic loading' line refers to a macroscopic modulus of 3.1 GPa. The deviation of the behaviour of the structure (of 455 atoms) from the loading line is due to its small size. (Courtesy of Professor U. W. Suter, ETH-Zürich)

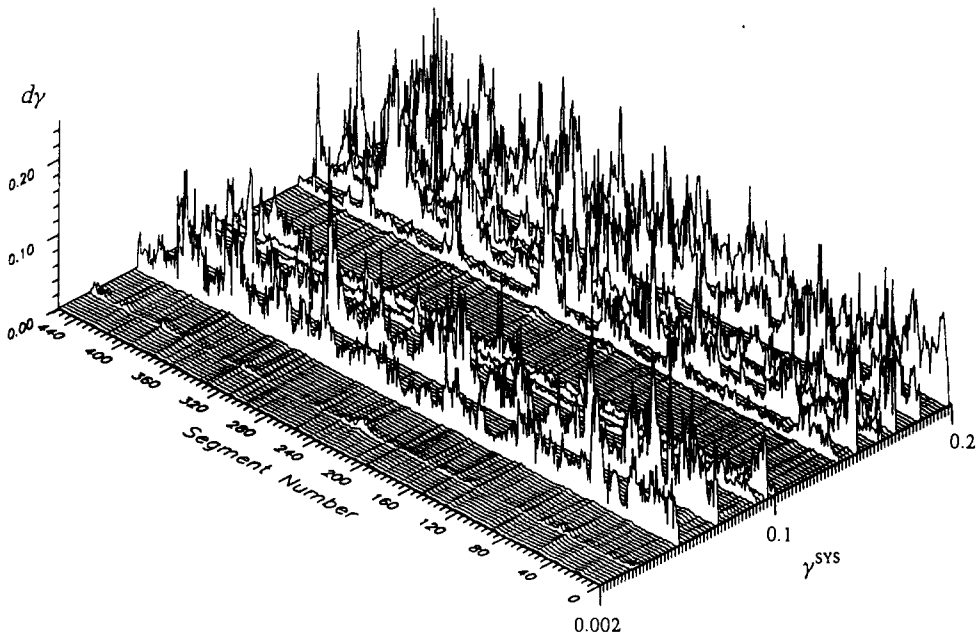

Figure 8 Incremental shear strain dγ of the effective segmental unit as a function of segment number and system strain as plotted in *Figure 7*. It is easily seen that segmental rearrangements (dγ) are never confined to just a few segments; they always affect hundreds of segments simultaneously. (Courtesy of Professor U. W. Suter, ETH-Zürich)

crank shaft motion; any plastic rearrangement invariably concerned 'hundreds of monomer units along the chain' (*Figure 8*). This is the third important conclusion to be drawn from such simulation experiments and it ties in extremely well with the previously described observations that it is not individual chain segments that are the orienting elements in a drawn glassy thermoplastic but volume elements of much larger size and, consequently, much smaller anisotropy[8].

Forces transmitted in (strong) flow

From the very beginning of polymer science, it was known that in a flowing solution forces are exchanged between a molecular chain and its liquid environment. These forces are frictional in nature, i.e. they depend on the rate of relative strain between the macromolecule and the surrounding liquid. In their classic experiments Keller and Odell[20] have shown that at increasing rates (elongational) strain forces are transmitted onto the coiled molecules which provoke their orientation, stretching and—at very high strain rates—even their scission[20]. In a dilute solution of PS in decalin scission of chains with $M_w \sim 10^6$ occurs at elongational strain rates of the order of $2 \times 10^5\ s^{-1}$ (ref. 21). In a recent article, Nguyen and Kausch[21] have reviewed the behaviour of molecular coils in stationary as well as in transient strong flow. They have especially pointed out a number of peculiar and as yet unexplained observations. Thus the frictional forces acting on a molecule are not linearly proportional to the zero shear rate solvent viscosity; in transient strong flow chains are not fully uncoiled before breakage but nevertheless they break with high precision in the centre. The latter observation is practically equivalent to assuming that tensile stresses can be transmitted through the chain backbone even in the presence of loops and kinks which leads to a maximum of axial chain loading and thus to preferred scission in the centre of the chain[21].

ENTANGLEMENT

In the previous section, the application of forces to a given chain segment in the solid state was discussed based on the assumption that the response of the segment in the solid state consists of a small strain elastic or plastic deformation. In either case, at such levels of deformation (up to 15%), the absence or presence of entanglements would not be felt by a given segment. At large plastic deformations however, and for $M > M_c$, where M_c is the molecular weight above which entanglement effects are observed in the melt, entanglement constraints may restrict further deformation. Entanglement is often modelled by considering the polymer to behave analogously to a crosslinked network. The notional crosslinks are termed entanglement points, and have a density in space ν_e. In terms of the molecular weight between entanglements, $M_e \sim M_c/2$:

$$\nu_e = N_A \rho / M_e \tag{3}$$

In an alternative description, the effect of the topological constraints is assumed to be to trap the polymer chain in a virtual tube of diameter d_e, equivalent to the spatial separation of entanglement points in the network model.

Analysis of rheological data in terms of such models allows the experimental determination of M_e, and has led to correlations between entanglement molecular weight and the characteristic ratio C_∞, such as[22]:

$$M_e = 3 M_b C_\infty^2 \tag{4}$$

where M_b is the molecular weight per bond. Attention must be paid to the fact that in this model entire groups in stiff chains are counted as one bond thus increasing M_b. Whilst the true situation may be too complex to be fully represented by a simple scaling law[23], equation (4) provides a reasonable empirical description of the experimental data.

If the entanglement network remains fixed during homogeneous shear deformation in the glassy state, the final extension ratio should be of the order of the natural draw ratio of the network, λ_{max}. λ_{max} is approximately the ratio of the chain contour length l_e between topologically linked entanglement points (in the network model), to their spatial separation d_e. The value of l_e is

given by $\alpha l_o M_e/M_o$, where α is a geometrical factor and l_o is the bond length, and d_e^2 may be estimated as $C_\infty n l_o^2 M_e/M_o$ (assuming a Gaussian configuration for the strands linking the entanglement points). Making use of equation (4):

$$\lambda_{max} = \alpha(M_e/C_\infty M_o)^{1/2} = \alpha(3C_\infty)^{1/2} \quad (5)$$

Since α is ~ 0.8, this gives $\lambda_{max} \sim 2.4$ for bisphenol A polycarbonate (PC) in which $C_\infty = 2.4$ and $\lambda_{max} \sim 4.38$ for PS for which $C_\infty = 10$. These are remarkably close to the measured draw ratios in these polymers[24]. Thus if one uses λ as a criterion for ductility, then in this case the more flexible chain leads to the less ductile polymer.

CRAZING

So far, the discussion of molecular processes has been limited to basic mechanical properties, namely elasticity, homogeneous shear deformation and chain scission. The question now arises as to how these elements combine in more complex processes such as those leading to macroscopic heterogeneous fracture.

Any general answer to such a question must involve discussion of crazing, which in amorphous polymers, frequently represents the link between microdeformation and macroscopic rupture. The craze morphology—that of a crack-like defect spanned by numerous highly drawn craze fibrils—may be explained in terms of the propagation of voids (as might be formed locally where patches of yielded material are constrained by the surrounding undeformed matrix), via a meniscus-type instability[25]. Both the rate of advance and the period of the instability, which will determine the eventual fibril separation, can be related to the surface energy of the advancing void tips. If this surface energy is large, it may be argued on either energetic or kinetic grounds that simple homogeneous shear deformation will be favoured over crazing[24].

Since the intrinsic Van der Waals surface energy varies relatively little from one polymer to another, one must look elsewhere in order to account for the contrasting behaviour of different amorphous polymers. It is observed that polymers such as PS, with low entanglement densities ($M_e = 18\,000$ and $\nu_e = 4 \times 10^{25}$), craze far more readily than highly entangled polymers such as PC ($M_e = 1500$ and $\nu_e = 30 \times 10^{25}$). This may be rationalized with reference to *Figure 9*. For voids to advance through an entangled polymer, entanglements must be lost. Hence in terms of the entanglement network model, strands linking entanglement points must be broken or disentangle by forced reptation. Well below the glass transition temperature (T_g), the frictional forces opposing forced reptation are higher than the scission force and chain scission is dominant. The void surface energy is then approximately:

$$\Gamma = \gamma + \frac{\Sigma U}{2} \quad (6)$$

where $\Sigma \sim \nu_e d_e/2$ is the number of entangled strands crossing unit surface area in the polymer in question, and U is the scission energy per bond. In PS, $\Sigma U/2$ is of the order of γ, but is up to an order of magnitude greater than γ in high entanglement density polymers such as PC, explaining why crazing is less favoured in the latter[24].

As the temperature is raised towards T_g, the monomeric friction coefficient may decrease sufficiently for forced reptation to replace scission[26–29]. This is most likely for low molecular weight chains and low strain rates, since disentanglement times are both relatively long, and strongly molecular weight dependent. In thin films this is manifested by a transition from shear to crazing in PC and poly(ether sulfone) (PES), which has a similar entanglement density to PC, and disentanglement has been invoked to account for the ductile–brittle transition in macroscopic tensile tests on PES[29]. Disentanglement has also been shown to occur in low molecular weight PS close to T_g[26,28].

There is evidence that these concepts may be extended to semicrystalline glassy polymers. Convenient examples of semicrystalline polymers are isotactic PS (iPS) and PC (which may be crystallized by prolonged exposure to solvent vapour). At very high undercoolings, it is not unreasonable to assume the entanglement densities of semicrystalline states of iPS and PC to be similar to those of their amorphous counterparts[30,31], and the same arguments as presented above may be used to explain certain aspects of their deformation behaviour; semicrystalline iPS crazes from room temperature up to T_g whereas in the same temperature range PC shows what is termed 'fibrillar shear' (*Figure 10*), which is the analogue of homogeneous shear in an amorphous polymer, the fibrillar texture resulting from the partial break-up of the lamellar structure of the undeformed material[32]. Disentanglement crazing is not seen in either case however, whence crystallinity appears to impede forced reptation. Indeed, selected area electron diffraction suggests strain induced crystallinity during crazing may also prevent disentanglement in amorphous iPS[31,33,34]. This is clearly not the case for amorphous PC, in which no evidence has been found for strain induced crystallinity, even during crazing at high temperature. However, amorphous thin films of another high entanglement density polymer, poly(ether ether ketone) (PEEK), which crystallizes more rapidly than PC, shows only homogeneous deformation even close to T_g[35].

Similar features to fibrillar shear are found in semicrystalline thin films of iPS, polypropylene (PP), PEEK and polyoxymethylene (POM) above their T_g[31,35,36]. However, deformation in the bulk may be associated with a much higher void content than in thin films, whence deformation zones at crack tips in rubbery semicrystalline polymers are also often referred to as crazes[37,38].

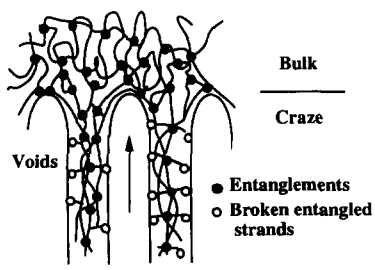

Figure 9 Schematic diagram of loss of entanglement by chain scission during void tip advance at the craze–bulk interface

FRACTURE IN AMORPHOUS GLASSY POLYMERS

It is generally held that crazing leads to brittleness. This is an oversimplification however, since in typical plane strain fracture mechanics specimens, relatively tough

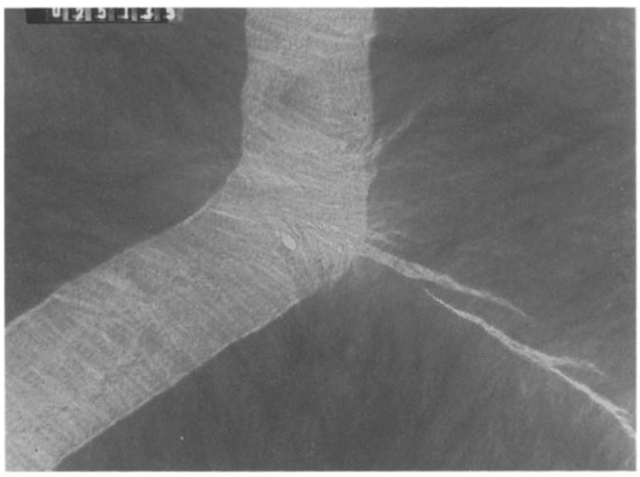

Figure 10 TEM micrograph of fibrillar shear in a thin film of semicrystalline polycarbonate deformed at room temperature

polymers such as PC and PES will also show crazing. This is reasonable, if one assumes the ultimate strength of the craze fibrils to be determined by Σ, the entangled strands being responsible for stress transfer. Hence craze fibrils in a highly entangled polymer such as PC should support higher stresses than a low entanglement density polymer.

In the case of a single craze propagating ahead of the crack during stable crack growth, Brown[39] equated the local crack driving force, g, for a crack propagating within a craze to the recoverable energy per unit area of the crack plane, $vS_c^2/2E_2$, where v is the craze thickness, E_2 is the modulus in the fibril direction and S_c is the mean stress at the craze–bulk interface. Since the craze can be considered as an orthotropic body:

$$g \sim k^2/(E_1E_2)^{1/2} \tag{7}$$

where E_1 is the modulus perpendicular to the fibrillar direction, assumed finite owing to the presence of cross-tie fibrils, and k is the local stress intensity at the crack tip. Since the effective crack opening displacement is given by $(1-1/\lambda)v$, in a macroscopic sample in which the small scale yielding (SSY) condition is satisfied, the fracture toughness G_{IC} may be written:

$$G_{IC} = (1-1/\lambda)vS_c \sim \frac{2(1-1/\lambda)k^2}{S_c}\left(\frac{E_2}{E_1}\right)^{1/2} \tag{8}$$

The local stress intensity at the crack tip is then argued to be determined by the fibril strength, giving $(\pi D_o)^{1/2}k = f_s\Sigma/2$, where D_o is a distance from the crack tip, assumed to equal the craze fibril spacing[39], f_s is the force required to break one such strand, whence $f_s\Sigma$ is approximately the breaking stress of one fibril. The final result is then:

$$G_{IC} = \frac{2\pi D_o}{S_c}\left(\frac{E_2}{E_1}\right)^{1/2}(1-1/\lambda)\frac{f_s\Sigma}{2} \tag{9}$$

Equation (9) has been shown to be consistent with data for stable crack propagation in PMMA, given reasonable estimates of the various quantities involved[39], and its essential correctness has been verified in detail by other workers[40]. Care should be taken when applying equation (9) quantitatively however, since it is only strictly valid for a single craze in stable propagation. Often multiple crazes and mixed shear and crazing may occur at crack tips, for example, all of which will contribute to energy dissipation.

FRACTURE IN SEMICRYSTALLINE POLYMERS ABOVE T_g

Measurements using compact tension specimens machined from compression and injection moulded plaques of POM show a systematic decrease in the plane-strain fracture toughness K_{IC} with crystallization temperature (T_c) and with molecular weight at low crosshead speeds, but little change in the yield stress in plane strain compression tests[41]. Under such conditions, a craze-like plastic deformation zone is clearly visible at the tip of the precrack, whence it may be argued on the basis of equation (9) that K_{IC} will be proportional to the effective value of Σ. One often refers to 'tie-molecules', which are molecular bridges between lamellae, when discussing semicrystalline polymers such as POM above T_g. However, since the proportion of true tie-molecules is likely to be relatively low, and given the apparently close analogies between the behaviour of semicrystalline polymers and that of their amorphous counterparts below T_g, we prefer to discuss Σ in terms of entanglements.

To account for the T_c and M dependence of K_{IC} in POM, we have estimated the degree of entanglement loss during crystallization in POM by using the Lauritzen–Hoffman secondary nucleation theory of spherulite growth[42]. At relatively high T_c (regime II, $T_c > 160$°C), there is evidence that forced reptation provides an adequate description of the growth kinetics, and it is argued that even at lower temperatures (regime III, $T_c < 160$°C), where growth occurs essentially by repeated nucleation of blocks of about three lamellar folds, reptation may still occur if there is sufficient time between nucleation events along a given chain, for it to attain a fully relaxed configuration. We have attempted to quantify this by assuming the chains to undergo reptation at their free ends, whilst allowing for the fact that loops of chain confined by nuclei will be unable to reptate, as shown in *Figure 11b*. Below ~140°C, nucleation is too rapid to allow even transient reptation, and so it is assumed that the entanglement density remains approximately that of the melt [entanglements may be rejected into the amorphous layers between lamellae, but only by 'reeling-in of slack' (*Figure 11a*) whence the effective tube length and hence the overall number of entanglements remains approximately constant].

Σ is taken to be proportional to the entanglement density v_e which is in turn estimated for $T > 140$°C from the mean amount by which the tube length diminishes in numerical simulations of the nucleation process[42]. The predicted evolution of K_{IC} with M and T_c is compared with experimental data in *Figure 12*. This approach accounts for the T_c dependence reasonably well, although it provides only a qualitative indication of the M dependence, which was assumed to arise both from the molecular weight dependence of entanglement loss and from chain end corrections to the final entanglement density. This may not only reflect shortcomings of the model, but also the fact that the experimental results are for highly polydisperse samples, whereas the model assumes monodispersity, and no attempt is made to take into account effects such as segregation according to chain length.

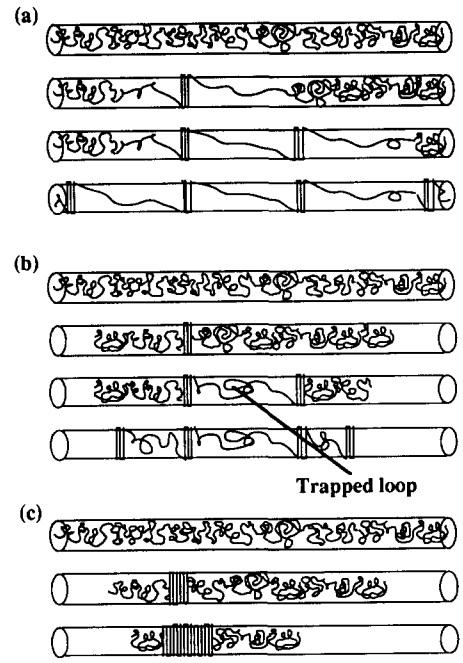

Figure 11 Schematic diagram of transport mechanisms during crystallization using the tube model (in each case the state of the chain after successive nucleation events is shown; note that in reality the tube will adopt a three-dimensional Gaussian configuration): (a) reeling-in of slack only; nucleation occurs too rapidly to allow full relaxation of the chain and so the tube length does not change as a result of chain folding; (b) reptation limited by multiple nucleation; the tube may shorten, but loops of amorphous chain pinned by multiple nuclei do not attain their equilibrium conformation; (iii) sideways growth of a single nucleus; no temporal or physical constraints on reptation

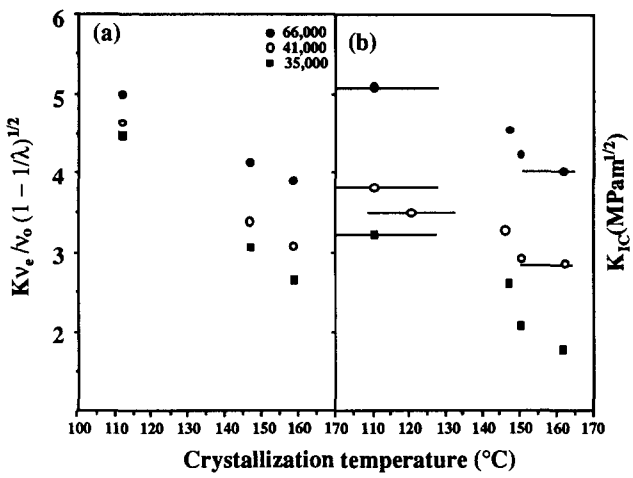

Figure 12 (a) Estimates of K_{IC} in POM from the entanglement density; K is chosen such that $K\nu_e/\nu_o[1/\lambda(\nu_e)]^{1/2}=5$ for $M_w=66\times10^3$ at the lowest crystallization temperature; (b) experimental K_{IC} behaviour at different crystallization temperatures and for different molecular weights

FRACTURE TOUGHNESS AND DIFFUSION ACROSS HOMOGENEOUS INTERFACES (CRACK HEALING)

It has long been recognized that development of joint strength must involve the establishment of entanglements across the interface when two surfaces of an amorphous uncrosslinked polymer are brought together. Evidence for this has been obtained for example, from studies[9,43,44] of fractured compact test specimens of PMMA, in which the fracture surfaces were brought together and heat treated above T_g. The subsequent evolution of the mechanical behaviour of the samples was M dependent, suggesting a diffusion process to be operating, and for a given M, K_{IC} increased as $t_h^{1/4}$, where t_h is the healing time, as confirmed by other authors[45]. Jud *et al.*[43] and Kausch and Jud[44] assumed the number of entanglements formed across the interface to be proportional to the contour length Δl diffused by the chains in time t_h. According to the models of DeGennes[46] and Doi and Edwards[47] for diffusion by reptation, $\langle\Delta l^2\rangle^{1/2}=2Dt_h$ where $D=kTM_o/\zeta_oM$ (ζ_o is the monomeric friction coefficient). Thus it was argued that the effective number of entanglements $n(t_h)$ in chains spanning the interface after time t_h is:

$$\frac{n(t_h)}{n(t_o)}=\left(\frac{t_h}{t_o}\right)^{1/2} \tag{10}$$

where t_o is the time to re-establish the K_{IC} of the sample prior to fracture. If it is then assumed that G_{IC} is proportional to n, equation (10) suggests K_{IC} to scale with $t_h^{1/4}$ consistent with the data[9,43,44].

This approach has paved the way for much subsequent discussion of the underlying mechanisms for the $t_h^{1/4}$ dependence of K_{IC}, and alternative mechanisms have been proposed by several authors. Since these have been reviewed elsewhere[9,43,48], we restrict ourselves here to some additional comments in the light of equation (9). PMMA crazes, whence equation (9) suggests G_{IC} ought to scale as Σ^2 and K_{IC} as Σ, which in turn suggests Σ to scale as $t_h^{1/4}$ rather than as $t_h^{1/2}$ as suggested above. In the case of a freshly fractured sample, the fracture surfaces will be covered with ruptured craze fibrils in which approximately half the entangled strands have been broken. The molecular weight distribution of the fibrils is highly polydisperse, with a molecular weight average M_{eff}, given by:

$$\frac{2}{M_{eff}}=\frac{1}{M_o}+\frac{1}{2M_e} \tag{11}$$

which is substantially less than the bulk molecular weight M_o[24]. The newly broken chain ends are likely to be concentrated at the fracture surface, under which conditions computer simulations have suggested that Σ should indeed vary as $t_h^{1/4}$ at an interface[49]. To see why this should be so in the present case, one might suppose that the density of chain ends at the fibril surfaces is $\sim2\Sigma$ since all the original strands crossing the surfaces will have been broken, and that less than half of these will begin to diffuse across the interface (some chains will diffuse away from the interface, and many pairs of chain ends are likely to belong to the same chain). Further, a considerable number of these chain ends will be associated with chain fragments too small to form entanglements and whose presence will have a significant diluting effect on the effective entanglement density even after partial diffusion[50].

In the bulk, the mean number of entangled strands crossing a planar surface per chain of molecular weight M intercepting that surface is approximately $(M/M_e)^{1/2}$. As previously, after time t_h the diffused molecular weight M_h will be proportional to $t_h^{1/2}$. Thus if one considers only diffusion of those chains whose ends are at the interface at $t_h=0$ and whose molecular weight is much greater than M_e, then $\Sigma(t_h)$ could be argued to increase as $(M_h/M_e)^{1/2}$ or as $t_h^{1/4}$, as long as the effective density of chain ends at the interface remains constant and is

very much less than Σ of the original interface. Whilst this is somewhat speculative, it does at least illustrate the point that whilst it should in principle be easy to distinguish between the different mechanisms by looking at the molecular weight dependence of K_{IC} at a given t_h, in practice the state of the interface is far from that of the bulk polymer whence it is difficult to know what molecular weight to take in calculating the effective diffusion constants[48].

FRACTURE TOUGHNESS OF HETEROGENEOUS INTERFACES

Perhaps a simpler system to model is that of an interface between two incompatible polymers A and B, made compatible by addition of a thin layer of diblock copolymer A_nB_n. On heat treatment the B blocks will migrate towards polymer B and the A block towards polymer A, so that the interface will be knitted together by the chemical bonds between the A and the B blocks. If one introduces a known quantity of block copolymer to the interface it should therefore be possible to calculate the effective value of Σ at the interface, with the proviso that at least one entanglement is needed between each block and its respective polymer to achieve effective reinforcement, as shown by Creton *et al.* for PS–polyvinylpyridine (PVP) interfaces[51].

Using this approach, Washiyama *et al.* have recently measured G_{IC} as a function of the areal chain density (effectively Σ) for PS-PVP block copolymers in which the PVP blocks were relatively short, using an asymmetric double cantilever beam geometry to ensure crack propagation along the interface[52]. TEM and forward recoil spectrometry permitted location of the PS half of the block after fracture. At a critical density Σ_c of 0.04 chains nm^{-2} they observed a transition from chain pull-out of the PVP blocks, to crazing of the PS side of the interface, associated with a discontinuous increase in G_{IC}. For longer PVP blocks on the other hand, pull-out was replaced by chain scission below Σ_c, as observed previously[53]. Since the crazing stress σ_c is known, identification of Σ_c in the respective cases and setting $\sigma_c = \Sigma_c f$, where f is the force either to break or disentangle a chain, allows one to estimate the monomeric friction coefficient and the force to break one bond, quantities which are of obvious fundamental importance[52,53]. That there is a change from a linear to a quadratic dependence of G_{IC} on Σ as suggested by equation (9) at the transition from simple cleavage to crazing (in cases where the crazes straddle the interface), has also been confirmed[39,53] by observations of the behaviour of interfaces with controlled Σ.

Similar considerations as discussed above apply to the bonding of rubbers, using a suitable polymer to make the interface compatible. The toughness again depends on Σ and in the case of rubbers is particularly sensitive to the deformation rate, which will in turn determine the extent of dissipative processes such as chain pull-out[54,55]. At very low deformation rates however, whilst pull-out is the dominant failure mechanism (unless the chains are chemically bonded[56]), it will contribute little to dissipation, being essentially a frictional effect, and below some critical crack opening rate v^* the interface shows only residual toughness. At higher crack opening rates, there is a transition to a regime in which pull-out begins to contribute to interface toughness, and the molecular bridges between the two interfaces become stretched as the deformation rate is increased, with chain scission eventually replacing pull-out at the highest deformation rates[55]. In intermediate regimes the extent of multiple crossing by a given connector becomes significant, since a high degree of multiple crossing will lead to an increased work of chain pull-out, which should lead to improvements in fracture toughness at a given deformation rate, as long as it does not provoke a transition to chain scission[27,55]. Much evidence for the role of chain pull-out in the toughening of rubber-bonded interfaces has been obtained from peel tests[57,58]. Use has also been made of the Johnson, Kendall, Roberts test to investigate bonding of crosslinked polyisoprene (PI) to PS using PS-PI block copolymers[55], confirming the toughness to increase linearly with crack speed above a threshold deformation rate in accordance with the pull-out models (here an elastic spherical cap is pressed into contact with a planar or spherical surface; on release of the applied load, the subsequent decrease in contact area with time will depend on the toughness of the interface).

CONCLUDING REMARKS

The anisotropic, chain-like nature of macromolecules has an important role in the static and dynamic interactions between chain segments. Special attention has been paid to the importance of three parameters:

- the nature and the periodicity of the attractive and repulsive interactions to which a chain segment is exposed and which strongly affect the level of forces to be transmitted and the response of the segment to such forces;
- the density of entanglements v_e and the areal density of entangled strands Σ which come to bear whenever a (molten or) solid polymer is deformed to beyond the limit of anelastic behaviour and which strongly influence the modes of adhesion, plastic deformation, and fracture;
- the role of the time-scales of deformation and relaxation: extended at high rates of strain a flexible chain in a thermoplastic polymer orients or breaks; under such conditions, even a molecular coil in dilute solution may behave as a glassy polymer.

ACKNOWLEDGEMENTS

The authors gratefully recognize the frequent discussions they had during the preparation of this paper with Professor A. Yee, Ann Arbor, Michigan, visiting professor at EPFL in 1992–1993 and Professor U. W. Suter, ETH-Zürich. They also acknowledge the financial support of this research by the Swiss National Science Foundation (FN) and the Commission pour l'encouragement de la recherche scientifique (CERS).

REFERENCES

1 Ward, I. M. *Proc. Phys. Soc.* 1962, **80**, 1176
2 Ward, I. M. 'Mechanical Properties of Solid Polymers', Wiley, London, 1971
3 Hadley, D. W. and Ward, I. M. in 'Structure and Properties of Oriented Polymers', (Ed. I. M. Ward), Applied Science Publishers, London, 1975
4 Hadley, D. W. and Ward, I. M. *Rep. Progr. Phys.* 1975, **38**, 1143
5 Ward, I. M. 'Developments in Oriented Polymers—1', Applied Science Publishers, London, 1982

6 Voigt, W. 'Lehrstuhl der Kristallphysik', Teubner, Leipzig, 1928, p. 410
7 Reuss, A. *Z. Angew. Math. Mech.* 1929, **9**, 49
8 Kausch-Blecken von Schmeling, H. H. *Kolloid Z.Z. Polym.* 1969, **234**, 1148; 1970, **237**, 251; *J. Polym. Sci.* 1971, **C32**, 1
9 Kausch, H. H. 'Polymer Fracture, Polymers Properties and Applications', Springer Verlag, Berlin, 1989
10 Kröner, E. 'Mikrostrukturmechanik, Tagung des GAMM-Fachausschusses Materialtheorie', GAMM, Stuttgart, 1992
11 Pantelides, S. T. *Phys. Today* 1992, September, 67
12 Blundell, D. J., Chivers, R. A., Curson, A. D., Love, J. C. and MacDonald, W. A. *Polymer* 1988, **29**, 1459
13 Troughton, M. J., Davies, G. R. and Ward, I. M. *Polymer* 1989, **30**, 58
14 Plummer, C. J. G. in 'Advanced Thermoplastic Composites: Characterization, Processing' (Ed. H. H. Kausch), Hanser, Munich, 1992, p. 227
15 Kausch, H. H. and Langbein, D. *J. Polym. Sci., Polym. Phys. Edn* 1973, **11**, 1201
16 Gibson, S. H., Holt, J. S. and Hope, P. S. *J. Polym. Sci., Polym. Phys. Edn* 1979, **A2**, 1375
17 Ludovice, P. J. and Suter, U. W. in 'Computational Modeling of Polymers' (Ed. J. Bicerano), M. Dekker, New York, 1992
18 Mott, P. H., Argon, A. S. and Suter, U. W. *Phil. Mag. A* 1993, **67**, 931
19 Argon, A. S. BP Chemicals Seminar Series in Polymer Science and Technology, Manchester, 1993
20 Keller, A. and Odell, J. *J. Colloid. Polym. Sci.* 1985, **263**, 181
21 Nguyen, T. Q. and Kausch, H. H. *Adv. Polym. Sci.* 1992, **100**, 73
22 Wu, S. *J. Polym. Sci.* 1989, **27**, 723
23 Richter, D., Farago, B., Butea, R., Fetters, L. J., Huang, J. S. and Ewen, B. *Macromolecules* 1993, **26**, 795
24 Kramer, E. J. *Adv. Polym. Sci.* 1983, **52/53**, 1
25 Argon, A. S. and Salama, M. M. *Mater. Sci. Eng.* 1977, **23**, 219
26 Kramer, E. J. and Berger, L. L. *Adv. Polym. Sci.* 1990, **91/92**, 1
27 McLeish, T. C. B., Plummer, C. J. G. and Donald, A. M. *Polymer* 1989, **30**, 1651
28 Donald, A. M. *J. Mater. Sci.* 1985, **20**, 2634
29 Plummer, C. J. G. and Donald, A. M. *J. Appl. Polym. Sci.* 1990, **41**, 1197
30 Morel, D. E. and Grubb, D. T. *Polymer* 1984, **25**, 417
31 Plummer, C. J. G., Cudré-Mauroux, N. and Kausch, H.-H. *J. Polym. Sci. Eng.* 1994, **34**, 318
32 More, A. P. and Donald, A. M. *Polymer* 1992, **33**, 4081
33 Morel, D. E. and Grubb, D. T. *J. Mater. Sci. Lett.* 1984, **3**, 5
34 Plummer, C. J. G. and Kausch, H.-H. *Polymer* 1993, **34**, 1972
35 Plummer, C. J. G. and Kausch, H.-H. *Polymer* 1993, **34**, 305
36 Plummer, C. J. G. unpublished results, 1993
37 Friedrich, K. *Adv. Polym. Sci.* 1983, **52/53**, 225
38 Narisawa, I. and Ishikawa, M. *Adv. Polym. Sci.* 1990, **91/92**, 353
39 Brown, H. R. *Macromolecules* 1991, **24**, 2752
40 Hui, C. Y., Ruina, A., Creton, C. and Kramer, E. J. *Macromolecules* 1992, **25**, 3948
41 Plummer, C. J. G., Menu, P., Cudré-Mauroux, N. and Kausch, H.-H. *J. Appl. Polym. Sci.* submitted
42 Lauritzen, J. I. and Hoffman, J. D. *J. Res. Natl. Bur. Std* 1960, **64A**, 73
43 Jud, K., Kausch, H.-H. and Williams, J. G. *J. Mater. Sci.* 1981, **16**, 204
44 Kausch, H.-H. and Jud, K. *Plast. Rubber Proc. Appl.* 1982, **2**, 265
45 Wool, R. P. and O'Connor, K. M. *J. Polym. Sci., Polym. Lett. Edn* 1982, **20**, 7
46 De Gennes, P. G. *J. Chem. Phys.* 1971, **55**, 572
47 Doi, M. and Edwards, S. F. *J. Chem. Soc. Faraday Trans. II* 1978, **74**, 1789
48 Tirrell, M. and Kausch, H.-H. *Ann. Rev. of Mat. Sci.* 1989, **19**, 341
49 Prager, S. and Tirrell, M. *J. Chem. Phys.* 1981, **73**, 5194
50 Plummer, C. J. G. and Donald, A. M. *J. Mater. Sci.* 1989, **24**, 1399
51 Creton, C., Kramer, E. J. and Hadziioannou, G. *Macromolecules* 1991, **24**, 1846
52 Washiyama, J., Kramer, E. J. and Hui, C.-Y. *Macromolecules* 1993, **26**, 2928
53 Creton, C., Kramer, E. J., Hui, C.-Y. and Brown, H. R. *Macromolecules* 1992, **25**, 3075
54 Brown, H. R. *Macromolecules* 1993, **26**, 1666
55 Hong, J. and de Gennes, P. G. *Macromolecules* 1992, **26**, 4002
56 de Gennes, P. G. *J. Phys. Fr.* 1989, **50**, 2551
57 Ellul, M. D. and Gent, A. N. *J. Polym. Sci., Polym. Phys. Edn* 1984, **22**, 1953
58 Reichert, W. F. and Brown, H. R. *Polymer* submitted